

Article

Leaf Age-Dependent Effects of Foliar-Sprayed CuZn Nanoparticles on Photosynthetic Efficiency and ROS Generation in *Arabidopsis thaliana*

Ilektra Sperdoui ^{1,2}, Julietta Moustaka ^{1,3}, Orestis Antonoglou ⁴,
Ioannis-Dimosthenis S. Adamakis ^{1,5}, Catherine Dendrinou-Samara ⁴ and
Michael Moustakas ^{1,*}

¹ Department of Botany, Aristotle University of Thessaloniki, GR-54124 Thessaloniki, Greece

² Institute of Plant Breeding and Genetic Resources, Hellenic Agricultural Organisation–Demeter, Thermi, GR-57001 Thessaloniki, Greece

³ Department of Plant and Environmental Sciences, University of Copenhagen, Thorvaldsensvej 40, DK-1871 Frederiksberg C, Denmark

⁴ Laboratory of Inorganic Chemistry, Department of Chemistry, Aristotle University of Thessaloniki, 54124 Thessaloniki, Greece

⁵ Department of Botany, Faculty of Biology, National and Kapodistrian University of Athens, 157 84 Athens, Greece

* Correspondence: moustak@bio.auth.gr; Tel.: +30-2310-99-8335

Received: 26 June 2019; Accepted: 3 August 2019; Published: 6 August 2019



Abstract: Young and mature leaves of *Arabidopsis thaliana* were exposed by foliar spray to 30 mg L⁻¹ of CuZn nanoparticles (NPs). The NPs were synthesized by a microwave-assisted polyol process and characterized by dynamic light scattering (DLS), X-ray diffraction (XRD), and transmission electron microscopy (TEM). CuZn NPs effects in *Arabidopsis* leaves were evaluated by chlorophyll fluorescence imaging analysis that revealed spatiotemporal heterogeneity of the quantum efficiency of PSII photochemistry (Φ_{PSII}) and the redox state of the plastoquinone (PQ) pool (q_p), measured 30 min, 90 min, 180 min, and 240 min after spraying. Photosystem II (PSII) function in young leaves was observed to be negatively influenced, especially 30 min after spraying, at which point increased H₂O₂ generation was correlated to the lower oxidized state of the PQ pool. Recovery of young leaves photosynthetic efficiency appeared only after 240 min of NPs spray when also the level of ROS accumulation was similar to control leaves. On the contrary, a beneficial effect on PSII function in mature leaves after 30 min of the CuZn NPs spray was observed, with increased Φ_{PSII} , an increased electron transport rate (ETR), decreased singlet oxygen (¹O₂) formation, and H₂O₂ production at the same level of control leaves. An explanation for this differential response is suggested.

Keywords: bimetallic nanoparticles; hydrogen peroxide; mature leaves; non-photochemical quenching; photoprotective mechanism; photosynthetic heterogeneity; plastoquinone pool; redox state; spatiotemporal heterogeneity; young leaves

1. Introduction

Both zinc (Zn) and copper (Cu) are essential elements for plant growth [1]. Zn deficiency results in a rapid inhibition of plant growth and development, while several physiological processes are impaired [1–3]. Zinc scarcity in arable soils [4] is a major problem worldwide [2], which is mainly due to the low Zn soil solubility resulting in Zn unavailability to plant roots [5]. Adequate Zn supply is suggested to improve productivity and nutrients in crops [6]. Low Zn concentrations in soils can be improved by adding Zn fertilizers, but this is a costly and ineffective policy [7]. However, to

increase grain Zn concentrations, foliar Zn application can be applied [7–9]. As Cu is also an essential element for all organisms, Cu-based fertilizers and fungicides have been widely used in agriculture as well [10,11].

Nanoparticles (NPs) in agriculture are used to reduce the amount of sprayed chemical products by the smart delivery of active ingredients, diminish nutrient losses in fertilization, and increase yields through optimized water and nutrient management [12–15]. Nevertheless, NPs are experiencing problems in reaching the market as novel products in agriculture, making agriculture still a negligible area for nanotechnology due mainly to the high production costs required in high volumes and to doubtful practical profits and lawmaking uncertainties [15]. In addition, the major concern regarding the use of NPs is their possible phytotoxicity, which is closely related to their chemical composition, structure, size, and surface area [12].

Since plant production is driven by photosynthesis, it is possible to estimate the fate of plant growth and development by evaluating photosynthetic function [16]. The process of photosynthesis converts light energy into chemical energy by the collaboration of photosystem I (PSI), and photosystem II (PSII), which work in coordination [16–18]. Chlorophyll fluorescence analysis has been widely used as a highly sensitive indicator of photosynthetic efficiency [19–26]. The obtained information can be interpreted to acquire knowledge about the state of the photosynthetic machinery and the effects of environmental pressure on plants [27,28]. Nevertheless, photosynthetic functioning is not uniform at the leaf area particularly under abiotic stress circumstances, which makes conventional chlorophyll fluorescence measurements non-characteristic of the physiological status of the entire leaf [29]. This disadvantage overcomes chlorophyll fluorescence imaging analysis and permits the detection of spatiotemporal heterogeneity at the total leaf surface [30–35].

The synthesis of hydrophilic CuZn NPs is challenging and has been hardly reported before [36,37]. We have previously evaluated the phytotoxicity of 15 mg L⁻¹ and 30 mg L⁻¹ of CuZn NPs sprayed on tomato plants by determining their effects on the light reactions of photosynthesis [38]. The evaluated CuZn NPs displayed minimal ionic dissolution (<10%), a significant amount of biocompatible polyol surface coating (32%), and high crystallinity, factors that minimize their toxic effects [39]. While no significant effects in PSII functionality were noticed with 15 mg L⁻¹ of NPs, the application of 30 mg L⁻¹ of CuZn NPs resulted in a reduced plastoquinone (PQ) pool that gave rise to H₂O₂ generation [38]. A reduced PQ pool reflects an imbalance between energy supply and demand [40,41]—or, in other words, excess excitation energy [42–44]. Young leaves have the ability to dissipate the excess excitation energy by non-photochemical quenching (NPQ) more efficiently than mature leaves [45], and this is sufficient in scavenging reactive oxygen species (ROS) [42,46,47]. Based on these reports, we hypothesized that exposing young and mature leaves to 30 mg L⁻¹ of CuZn NPs will result in differential effects on them, with young leaves retaining a more oxidized PQ pool and less H₂O₂ accumulation. *Arabidopsis thaliana* was selected as the plant material to test our hypothesis, since it has been widely used as a model system in understanding the physiological mechanisms of higher plants [31,48].

2. Materials and Methods

2.1. Synthesis of CuZn NPs

Based on our previous results, a modified synthesis of CuZn NPs was followed using a commercial microwave accelerated reaction system, the Model MARS 6-240/50-CEM [38]. Equal amounts of Zn(NO₃)₂·4H₂O (2.0 mmol) and Cu(NO₃)₂·3H₂O (2.0 mmol) were mixed and dissolved in 20 mL of triethylene glycol (TrEG). After centrifugation at 2800 g, the supernatant liquids were discarded, and the black-brown precipitate was washed three times with ethanol. NPs were re-dispersed in water via sonication assistance to form stable aqueous suspensions at concentrations <200 mg L⁻¹.

2.2. Characterization of CuZn NPs

Primary particle size and morphology was determined by a conventional transmission electron microscope (TEM) (JEOL JEM 1010, Tokyo, Japan) [38].

The crystal structure was investigated through X-ray diffraction (XRD) performed on a Philips PW 1820 diffractometer (Amsterdam, The Netherlands) at a scanning rate of 0.050/3 s, in the 2θ range from 10° to 90° , with monochromatized Cu K α radiation ($\lambda = 1.5406$ nm) [38].

The hydrodynamic size of CuZn NPs was determined by dynamic light scattering (DLS) measurements, which were carried out at 25°C utilizing a Nano ZS Zetasizer (Malvern Instrument, Worcestershire, UK) apparatus [33].

2.3. Plant Material and Exposure to CuZn NPs

Arabidopsis thaliana ecotype Columbia (Col-0) seeds obtained from the Nottingham Arabidopsis Stock Centre (NASC) were sown on a soil and peat mixture in a controlled-environment growth chamber under $22 \pm 1/18 \pm 1^\circ\text{C}$ day/night temperature with a 16-hour day at $130 \pm 20 \mu\text{mol photons m}^{-2} \text{s}^{-1}$ light intensity and $50 \pm 5/60 \pm 5\%$ day/night humidity. Four and six-week-old Arabidopsis plants were sprayed with 30 mg L^{-1} of CuZn NPs. Rosette leaf 8 from four-week-old (young, immature leaf) and six-week-old (mature to senescing leaf) were selected for photosynthetic measurements 30 min, 90 min, 180 min, and 240 min after the foliar spray with 30 mg L^{-1} of CuZn NPs, while control plants were sprayed with distilled water.

2.4. Chlorophyll Fluorescence Imaging Analysis

Chlorophyll fluorescence analysis was conducted with an Imaging-PAM Chlorophyll Fluorometer (Walz, Effeltrich, Germany) as described in detail previously [27]. Chlorophyll fluorescence parameters were measured in dark-adapted (15 min) leaves (rosette leaf 8) from four and six-week-old Arabidopsis plants sprayed with distilled water (control), or 30 mg L^{-1} of CuZn NPs. In each leaf, eight to 11 areas of interest (AOI) that covered the whole leaf area were selected for analysis. Four to five leaves from different plants were measured at each treatment at the actinic light intensity of $140 \mu\text{mol photons m}^{-2} \text{s}^{-1}$. By using the Imaging Win software (Heinz Walz GmbH, Effeltrich, Germany), we measured the effective quantum yield of photochemistry in PSII (Φ_{PSII}), the quantum yield of regulated non-photochemical energy loss in PSII (Φ_{NPQ}), the quantum yield of non-regulated energy loss in PSII (Φ_{NO}), the photochemical quenching (q_p) that is a measure of the redox state of the PQ pool, the non-photochemical quenching (NPQ), and the relative PSII electron transport rate (ETR).

Representative results of the effective quantum yield of photochemical energy conversion in PSII (Φ_{PSII}) and the redox state of PQ pool (q_p) are also shown as color-coded images, after 5 min of illumination with $140 \mu\text{mol photons m}^{-2} \text{s}^{-1}$.

2.5. Imaging of ROS

The presence of ROS was detected in young and mature leaves of *Arabidopsis thaliana* by staining with $25 \mu\text{M}$ of 2',7'-dichlorofluorescein diacetate ($\text{H}_2\text{DCF-DA}$, Sigma, St. Louis, MO, USA) in the dark, as described before [41]. After 30 min of incubation, the leaves were observed with a Zeiss AxioImager Z.2 fluorescence microscope (Jena, Germany) equipped with an MRc5 Axiocam using the AxioVision SE64 4.8.3 software according to the manufacturer's instructions.

2.6. Statistical Analyses

Four to five leaves from different plants were analyzed for each treatment, and the differences between chlorophyll fluorescence parameters were separated by paired t-test at a level of $p < 0.05$ with the StatView software (computer package, Abacus Concepts, Inc., Berkeley, CA, USA) [23].

3. Results

3.1. Characterization of the Synthesized CuZn NPs

The crystal structure of the NPs was investigated through X-ray diffraction (XRD) (Figure 1a). The observed peaks at 35.84° , 42.4° , 49.78° , and 73.47° are attributed to γ -brass (JCPDS no. 5-6566) and α -brass (JCPDS no. 50-1333 and no. 65-6567), while no significant changes were observed from the previous reported by us CuZn NPs [38]. The composition analysis of the NPs by inductively coupled plasma (ICP) indicated a 52%/48% copper/zinc proportion, respectively, and thus an overall composition of α -Cu₄₇Zn₂₉/ γ -Cu₉Zn₁₅ based on the X-ray diffractions. TEM images of CuZn NPs (Figure 2) revealed small, spherical nanoparticles in the range of 20 nm to 30 nm in contrast to the formation of nanoclusters [38]. The different nanoarchitecture is attributed to the half amount of polyol (TrEG) that has been used in the present synthesis.

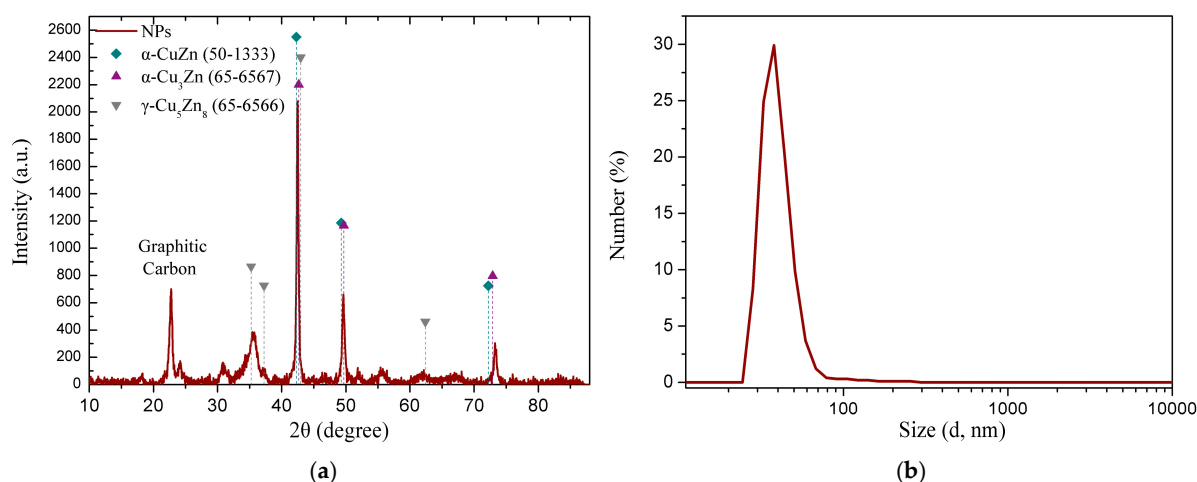


Figure 1. The X-ray diffraction (XRD) patterns of CuZn nanoparticles (NPs) (a), and the size distribution (diameter in nm) of the aqueous suspensions of CuZn NPs evaluated by dynamic light scattering (DLS) numbers measurements (b).

CuZn NPs are hydrophilic, and thus readily disperse in water. The hydrodynamic diameter provided by DLS number measurements (Figure 1b) was 35 nm, matching well to the size provided by TEM and indicated monodispersity. Additionally, the amount of leached ions in a 30 mg L^{-1} aqueous suspension of CuZn NPs after 24 h of incubation was found to be 1.8 mg L^{-1} for Cu and 2.2 mg L^{-1} for Zn, respectively.

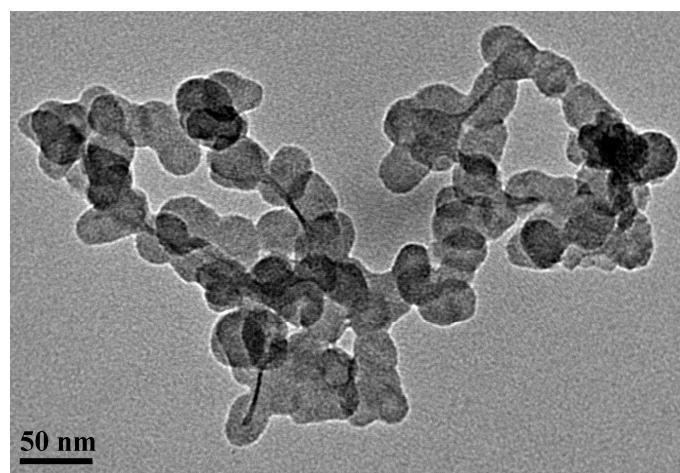


Figure 2. Size and morphology of CuZn NPs determined by transmission electron microscopy.

3.2. Changes in Light Energy Partitioning at PSII in Young and Mature Leaves After Exposure to CuZn NPs

We estimated the light energy partitioning at PSII, that is, Φ_{PSII} , Φ_{NPQ} and Φ_{NO} , which sum to one. The quantum yield of photochemical energy conversion (Φ_{PSII}) at 30 min, 90 min, and 180 min after the foliar spray with 30 mg L⁻¹ of CuZn NPs presented a significant decrease in young leaves, while in mature leaves, it increased significantly compared to controls (Figure 3a). Φ_{PSII} recovered to control values in young leaves 240 min after the spray, while at the same time remaining significantly higher than controls in mature leaves (Figure 3a). Φ_{PSII} in mature leaves at 30 min, 90 min, 180 min, and 240 min after spraying with CuZn NPs was significantly higher than young leaves (Figure 3a).

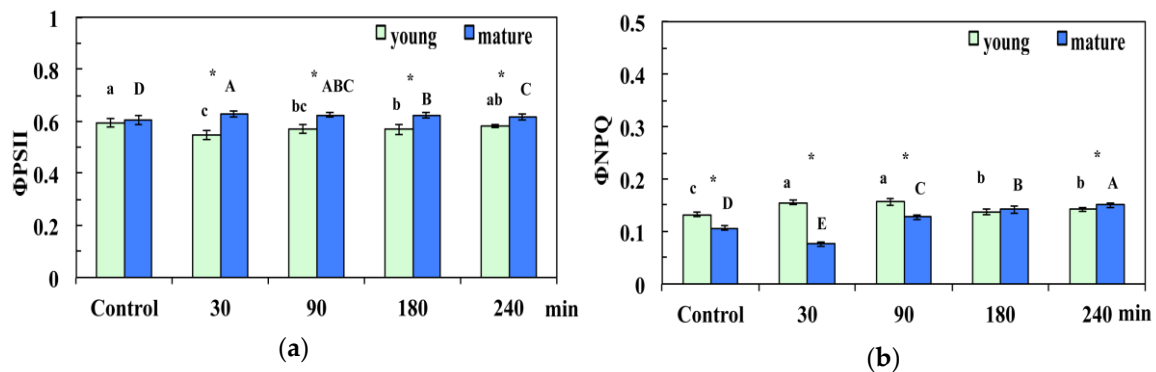


Figure 3. Changes in the quantum efficiency of photosystem II (PSII) photochemistry (Φ_{PSII}) (a), and the quantum yield of regulated non-photochemical energy loss in PSII (Φ_{NPQ}) (b); of *Arabidopsis thaliana* young and mature leaves measured (at 140 $\mu\text{mol photons m}^{-2} \text{s}^{-1}$) 30 min, 90 min, 180 min, and 240 min after the foliar spray with 30 mg L⁻¹ of CuZn NPs or distilled water (control). Error bars on columns are standard deviations based on four to five leaves from different plants. Columns with different letters (lowercase for young leaves and capitals for mature) are statistically different ($p < 0.05$). An asterisk (*) represents a significantly different mean of the same time treatment between young and mature leaves ($p < 0.05$).

The quantum yield of regulated non-photochemical energy loss (Φ_{NPQ}) at 30 min, 90 min, 180 min, and 240 min after the CuZn NPs spray increased significantly, compared to control, in young leaves (Figure 3b). Φ_{NPQ} 30 min after the NPs spray decreased in mature leaves, while it increased significantly afterwards, compared to control (Figure 3b). Φ_{NPQ} in young control leaves, and at 30 min and 90 min after the CuZn NPs spray was significantly higher than that in mature leaves (Figure 3b). In comparison, Φ_{NPQ} was significantly higher in mature leaves 240 min after the spray with CuZn NPs (Figure 3b).

The quantum yield of non-regulated energy loss (Φ_{NO}), which is a loss process due to PSII inactivity, increased significantly in young leaves 30 min after the CuZn NPs spray compared to control, while it remained unchanged in mature leaves, where it decreased significantly later on (90 min, 180 min, and 240 min after the foliar spray) (Figure 4). In young leaves, Φ_{NO} 90 min after the foliar spray with NPs decreased to control values, and increased later on (180 min), but retained control values 240 min after spraying with the NPs (Figure 4). Φ_{NO} in mature control leaves was significantly higher than that in young leaves, but at 90 min, 180 min, and 240 min after the foliar spray with 30 mg L⁻¹ of CuZn NPs, it decreased significantly compared to young leaves and control values (Figure 4).

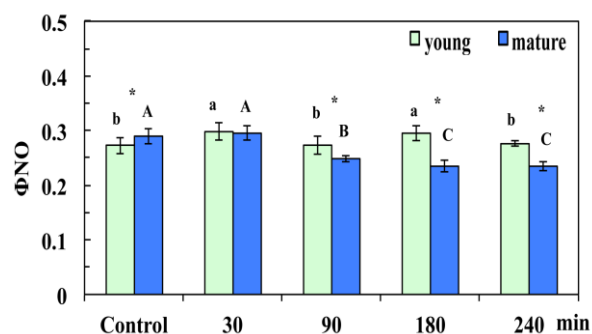


Figure 4. Changes in the quantum yield of non-regulated energy dissipation in PSII (Φ_{NO}) of *Arabidopsis thaliana* young and mature leaves measured (at $140 \mu\text{mol photons m}^{-2} \text{s}^{-1}$) 30 min, 90 min, 180 min, and 240 min after the foliar spray with 30 mg L^{-1} of CuZn NPs or distilled water (control). Error bars on columns are standard deviations based on four to five leaves from different plants. Columns with different letter (lower case for young leaves and capitals for mature) are statistically different ($p < 0.05$). An asterisk (*) represents a significantly different mean of the same time treatment between young and mature leaves ($p < 0.05$).

3.3. Changes in the Photoprotective Energy Dissipation and the Electron Transport Rate in Young and Mature Leaves After Exposure to CuZn NPs

The non-photochemical quenching (NPQ) increased significantly at 30 min and 90 min after the CuZn NPs spray in young leaves, compared to the control, while it decreased 180 min after spraying, and increased again significantly 240 min after spraying (Figure 5a). NPQ in mature leaves decreased 30 min after spraying with NPs, but later on (90 min, 180 min, and 240 min after the foliar spray), it increased compared to control values (Figure 5a). NPQ was significantly higher in young leaves compared to mature and control leaves and 30 min and 90 min after the CuZn NPs spray, but significantly lower than in mature leaves at 180 min and 240 min after the foliar spray (Figure 5a).

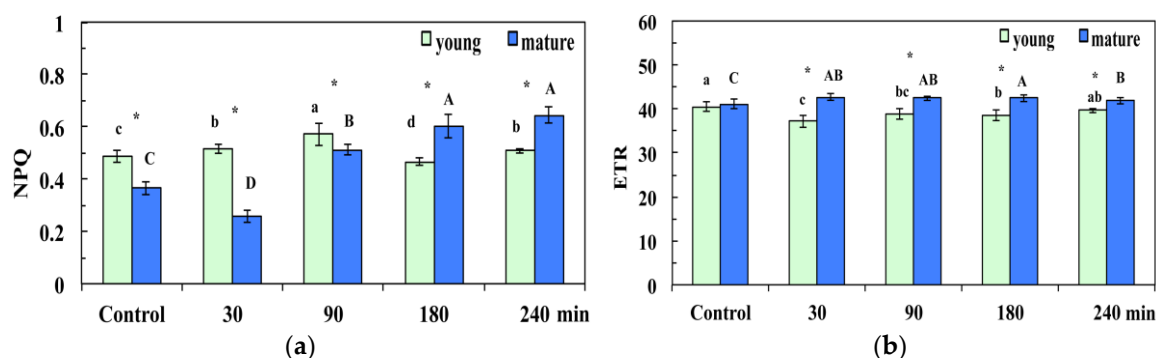


Figure 5. Changes in the non-photochemical fluorescence quenching (NPQ) (a), and the relative PSII electron transport rate (ETR) (b); of *Arabidopsis thaliana* young and mature leaves measured (at $140 \mu\text{mol photons m}^{-2} \text{s}^{-1}$) 30 min, 90 min, 180 min, and 240 min after the foliar spray with 30 mg L^{-1} of CuZn NPs or distilled water (control). Error bars on columns are standard deviations based on four to five leaves from different plants. Columns with different letter (lower case for young leaves and capitals for mature) are statistically different ($p < 0.05$). An asterisk (*) represents a significantly different mean of the same time treatment between young and mature leaves ($p < 0.05$).

The relative electron transport rate at PSII (ETR) decreased significantly in young leaves 30 min, 90 min, and 180 min after the foliar spray with 30 mg L^{-1} of CuZn NPs, while at the same time it increased significantly in mature leaves compared to controls (Figure 5b). ETR recovered to control values in young leaves 240 min after the spray, while it remained significantly higher than controls in mature leaves (Figure 5b). The ETR in mature leaves at 30 min, 90 min, 180 min, and 240 min after the spray with CuZn NPs was significantly higher than that in young leaves (Figure 5b).

3.4. Changes in the Redox State of Plastoquinone (PQ) Pool in Young and Mature Leaves After Exposure to CuZn NPs

The redox state of PQ pool (q_p), which is a measure of the fraction of open PSII reaction centers, decreased significantly at 30 min and 180 min after the CuZn NPs spray in young leaves, compared to control; in contrast, it was at control values 90 min and 240 min after spraying (Figure 6).

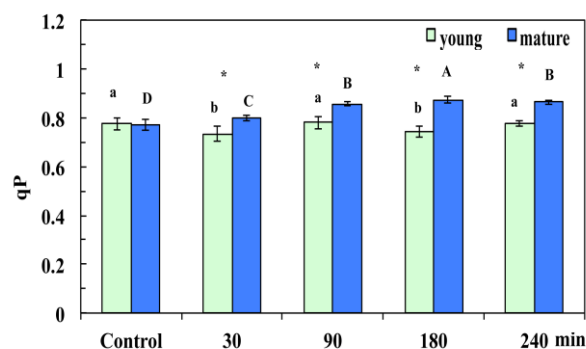


Figure 6. Changes in the photochemical fluorescence quenching, which is the relative reduction state of the plastoquinone (PQ) pool, reflecting the fraction of open PSII reaction centers (q_p) of young and mature *Arabidopsis thaliana* leaves measured (at $140 \mu\text{mol photons m}^{-2} \text{s}^{-1}$) 30 min, 90 min, 180 min, and 240 min after the foliar spray with 30 mg L^{-1} of CuZn NPs or distilled water (control). Error bars on columns are standard deviations based on four to five leaves from different plants. Columns with different letter (lower case for young leaves and capitals for mature) are statistically different ($p < 0.05$). An asterisk (*) represents a significantly different mean of the same time treatment between young and mature leaves ($p < 0.05$).

At all the sampling periods (30 min, 90 min, 180 min, and 240 min after the NPs spray), the mature leaves were in a more oxidized state than control (Figure 6).

3.5. Spatiotemporal Heterogeneity of the Quantum Efficiency of PSII Photochemistry and the Redox State of Plastoquinone (PQ) Pool in Young and Mature Leaves After Exposure to CuZn NPs

The quantum yield of photochemical energy conversion (Φ_{PSII}) in control young leaves showed a spatial heterogeneity, with higher values in the midrib of the leaves than in the lamina (Figure 7a). A spatiotemporal heterogeneity of Φ_{PSII} in young leaves was evident 30 min after the foliar spray with 30 mg L^{-1} of CuZn NPs with lower values in the distal (tip) leaf area (Figure 7b). The spatiotemporal heterogeneity of Φ_{PSII} in young leaves 90 min after the foliar spray was still evident due to an increase of whole leaf Φ_{PSII} values (Figure 7c), and became amplified 180 min after spraying (Figure 7d). Then, 240 min after spraying with CuZn NPs, Φ_{PSII} increased to the control whole leaf values, showing also a spatial heterogeneity, with higher Φ_{PSII} values in the area where lower values were previously scored (distal leaf area) (Figure 7e).

Mature control leaves (Figure 8a) presented less spatial heterogeneity in Φ_{PSII} compared to control young leaves (Figure 7a), with higher values in the distal (tip) leaf area (Figure 8a). Higher values also occurred in the same area 30 min after the foliar spray with 30 mg L^{-1} CuZn NPs, which also caused the whole leaf Φ_{PSII} to increase (Figure 8b). The spatiotemporal heterogeneity of Φ_{PSII} in mature leaves was also evident 90 min after spraying with NPs (Figure 8c), but become less apparent 180 min after the foliar spray (Figure 8d). At 240 min after the foliar spray, Φ_{PSII} decreased in mature leaves in the whole leaf area, but remained higher than in the control leaves (Figure 8e).

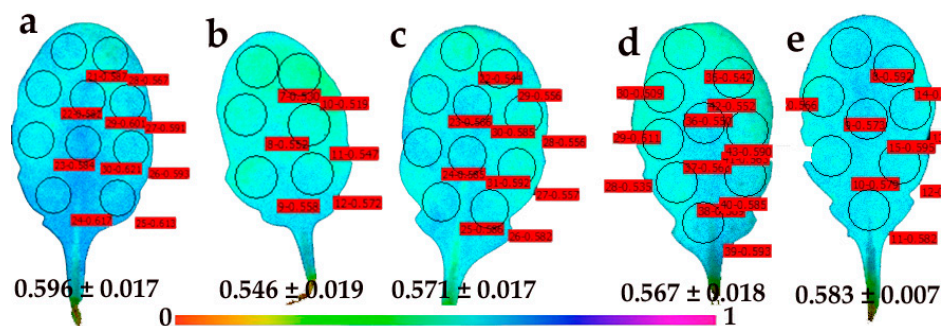


Figure 7. Representative chlorophyll fluorescence images of the effective quantum yield of PSII photochemistry (Φ_{PSII}) of *Arabidopsis thaliana* young leaves after 5 min of illumination at $140 \mu\text{mol photons m}^{-2} \text{s}^{-1}$. Leaves were measured after the foliar spray with distilled water (control) (a), or 30 min (b), 90 min (c), 180 min (d) and 240 min (e) after the foliar spray with 30 mg L^{-1} of CuZn NPs. The color code depicted at the bottom of the images ranges from values 0.0 to 1.0. The areas of interest (AOI) are shown in each image. The average Φ_{PSII} value of all the AOI for the whole leaf is shown.

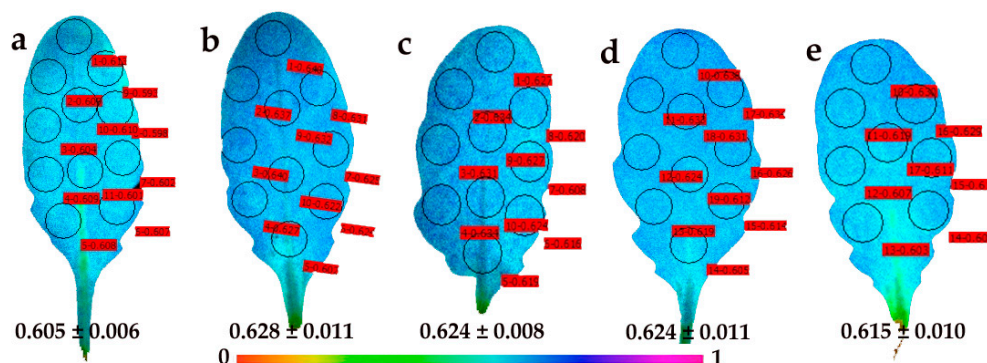


Figure 8. Representative chlorophyll fluorescence images of the effective quantum yield of PSII photochemistry (Φ_{PSII}) of *Arabidopsis thaliana* mature leaves after 5 min of illumination at $140 \mu\text{mol photons m}^{-2} \text{s}^{-1}$. Leaves were measured after the foliar spray with distilled water (control) (a), or 30 min (b), 90 min (c), 180 min (d) and 240 min (e) after the foliar spray with 30 mg L^{-1} of CuZn NPs. The color code depicted at the bottom of the images ranges from values 0.0 to 1.0. The areas of interest (AOI) are shown in each image. The average Φ_{PSII} value of all the AOI for the whole leaf is shown.

Images of the redox state of the PQ pool (q_P) of control young leaves showed a spatial heterogeneity, with higher values in the proximal (base) midrib of leaves (Figure 9a), as observed in the images of Φ_{PSII} (Figure 7a). At 30 min after the foliar spray with 30 mg L^{-1} of CuZn NPs, a spatiotemporal heterogeneity of q_P in young leaves was noticed, with lower values in the distal (tip) leaf area (Figure 9b) and significantly lower whole leaf q_P values than those of the young control leaves (Figure 9a). At 90 min after the foliar spray with CuZn NPs, the q_P images of young leaves (Figure 9c) were similar to the images of control young leaves (Figure 9a). At 180 min after the foliar spray with CuZn NPs, the whole leaf q_P values in young leaves decreased (Figure 9d), resembling the images 90 min after the foliar spray (Figure 9c) with less evident heterogeneity. At 240 min after spraying with NPs, whole leaf q_P values (Figure 9e) resemble those of control young leaves (Figure 9a).

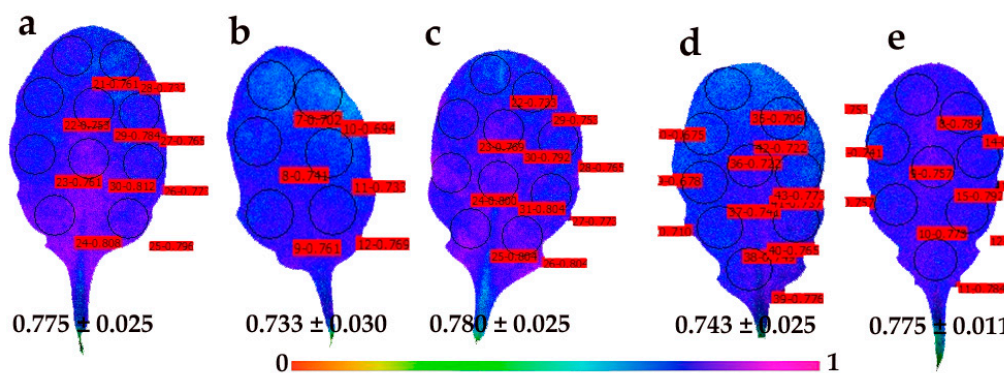


Figure 9. Representative chlorophyll fluorescence images of the relative reduction state of the plastoquinone (PQ) pool, that is, the photochemical fluorescence quenching, reflecting the fraction of open PSII reaction centers (q_p), of *Arabidopsis thaliana* young leaves after 5 min of illumination at $140 \mu\text{mol photons m}^{-2} \text{s}^{-1}$. Leaves were measured after the foliar spray with distilled water (control) (a), or 30 min (b), 90 min (c), 180 min (d), and 240 min (e) after the foliar spray with 30 mg L^{-1} of CuZn NPs. The color code depicted at the bottom of the images ranges from values 0.0 to 1.0. The areas of interest (AOI) are shown in each image. The average q_p value of all the AOI for the whole leaf is shown.

Images of the redox state of the PQ pool (q_p) of control mature leaves showed leaf homogeneity rather than leaf heterogeneity (Figure 10a). At 30 min after the foliar spray with 30 mg L^{-1} of CuZn NPs, a slight heterogeneity of q_p was observed in mature leaves, with increased q_p values in the whole leaf area (Figure 10b). Later on (90 min, 180 min, and 240 min after spraying with CuZn NPs), a further increase of q_p values compared to the control mature leaves was observed in the whole leaf area (Figure 10c–e).

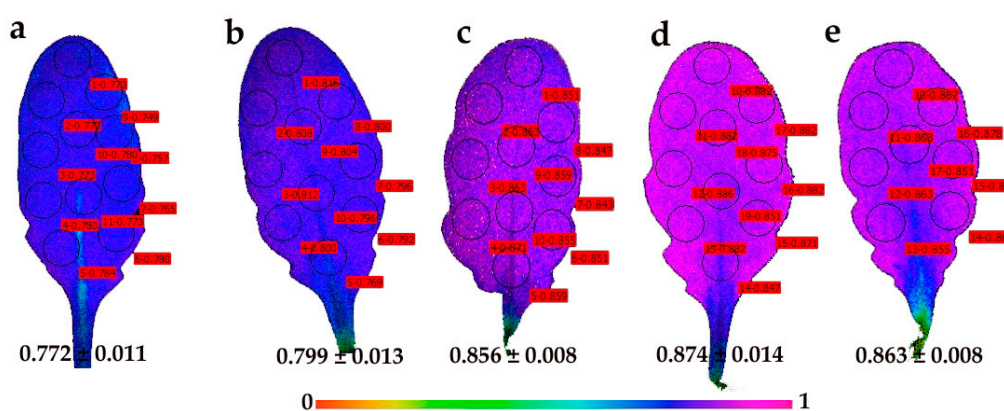


Figure 10. Representative chlorophyll fluorescence images of the relative reduction state of the plastoquinone (PQ) pool—that is, the photochemical fluorescence quenching, reflecting the fraction of open PSII reaction centers (q_p) of *Arabidopsis thaliana* mature leaves after 5 min of illumination at $140 \mu\text{mol photons m}^{-2} \text{s}^{-1}$. Leaves were measured after the foliar spray with distilled water (control) (a), or 30 min (b), 90 min (c), 180 min (d) and 240 min (e) after the foliar spray with 30 mg L^{-1} of CuZn NPs. The color code depicted at the bottom of the images ranges from values 0.0 to 1.0. The areas of interest (AOI) are shown in each image. The average q_p value of all the AOI for the whole leaf is shown.

3.6. ROS Generation in Young and Mature Leaves After Exposure to CuZn NPs

ROS generation was quantified in young (Figure 11a–e) and mature (Figure 11f–j) *A. thaliana* leaves by the fluorescent probe DCF-DA. In both young (Figure 11a) and mature (Figure 11f) control leaves, no notable quantities of H_2O_2 could be observed. At 30 min after the foliar spray with CuZn NPs, the highest H_2O_2 generation was noticed in young leaves (Figure 11b), accompanying the lower measured q_p values (Figure 9b). At the same time in mature leaves (Figure 11g), the level of ROS accumulation was similar to the control values (Figure 11f). At 90 min after the CuZn NPs spray, almost

no H_2O_2 could be detected in young leaves (Figure 11c). In mature leaves, no H_2O_2 could be detected at 90 min, 180 min, and 240 min after the CuZn NPs spray, either (Figure 11h–j). At 180 min after spraying with CuZn NPs, a high H_2O_2 production (but substantially less than 30 min after spraying) was observed in young leaves (Figure 11d). At 240 min after spraying with CuZn NPs, the level of ROS accumulation in young leaves (Figure 11e) was similar to that of the control (Figure 11a).

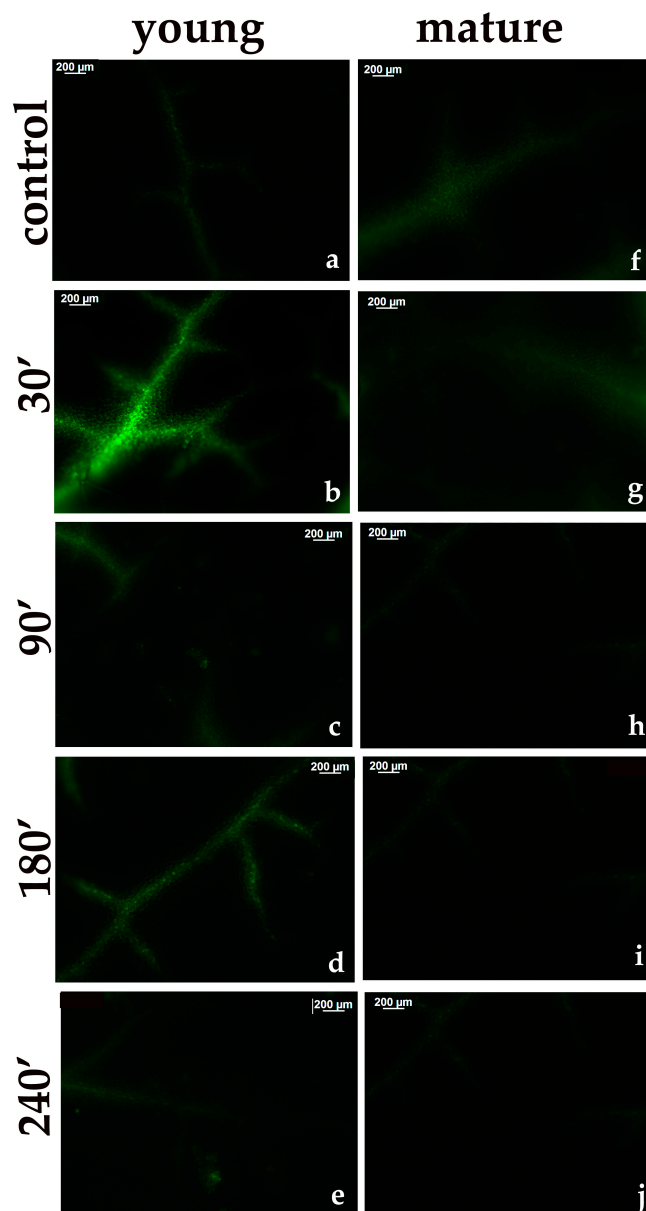


Figure 11. Representative patterns of reactive oxygen species (ROS) (H_2O_2) production in *Arabidopsis thaliana* young (a–e) and mature (f–j) leaves, as indicated by the fluorescence of $\text{H}_2\text{DCF-DA}$. The H_2O_2 generation after the foliar spray with distilled water (control) in a young leaf (a) and mature leaf (f); or 30 min after foliar spray with 30 mg L^{-1} of CuZn NPs in a young leaf (b) and mature leaf (g); 90 min after foliar spray with 30 mg L^{-1} of CuZn NPs in a young leaf (c) and mature leaf (h); 180 min after foliar spray with 30 mg L^{-1} of CuZn NPs in a young leaf (d) and mature leaf (i); and 240 min after foliar spray with 30 mg L^{-1} of CuZn NPs in a young leaf (e), and mature leaf (j). Scale bare: $200 \mu\text{m}$. A higher H_2O_2 content is indicated by the light green color.

4. Discussion

Inorganic NPs are emerging as novel agrochemicals due to their unique characteristics and high surface energy, which make them effective in lower doses compared to conventional inorganic ionic formulations. For instance, bulk brass has been utilized in the healthcare industry, while ionic forms of zinc and copper such as Bordeaux mixture, sulfate, and chloride salts are used in agrochemistry, but with adverse environmental effects and toxicity. However, due to the low water solubility, these ionic forms of agrochemicals are applied in relatively large amounts in order to effectively control the phytopathogens when the spores vegetate, which is through causing the secretion of malic acid and amino acids and subsequently dissolving them [49]. As a consequence, the limit between plant protection and phytotoxicity is still a matter of discussion. A need exists for new products that are going to have high biological activity and less metal in the formulation. Under these perspectives, hydrophilic CuZn NPs retain the desired characteristics of bulk brass, while forming stable aqueous suspensions with minimal ionic dissolution that are effective in low doses.

Young leaves can utilize only a fraction of absorbed irradiance in photochemical reactions via CO₂ assimilation, since light capture ability develops earlier than CO₂ assimilation capacity [45,50,51]. When the absorbed light is not used in photochemistry, in order to avoid photodamage, the excess excitation energy has to be safely removed by a photoprotective mechanism called non-photochemical quenching (NPQ) [52,53]. Consequently, the ability to dissipate excess excitation energy by NPQ is higher in young leaves than in mature leaves [45,47], which means that under control growth conditions, NPQ is significantly higher in young leaves compared to mature leaves (Figure 5a).

Heterogeneity in PSII photochemistry has been frequently reported to depend on the leaf age [41–43,45,47,48]. We observed changes in light energy partitioning related to leaf age under control growth conditions mostly related to Φ_{NPQ} and Φ_{NO} . Control young leaves had higher Φ_{NPQ} than mature leaves (Figure 3b), and without any significant difference in Φ_{PSII} (Figure 3a), it resulted in significantly lower Φ_{NO} (Figure 4). However, 90 min, 180 min, and 240 min after the NPs spray, Φ_{NO} increased in young leaves compared to mature leaves (Figure 4) due to a decreased photochemical energy conversion (Φ_{PSII}) (Figure 3a) that could not be compensated by the increased Φ_{NPQ} (Figure 3b). Φ_{NO} consists of chlorophyll fluorescence internal conversions and intersystem crossing, which leads to the formation of singlet oxygen (¹O₂) via the triplet state of chlorophyll (³chl*) [41,54–56], thus suggesting increased ¹O₂ formation in young leaves compared to mature leaves. NPQ is one of the most important photoprotective mechanisms in plants [25,41,57,58]. The enhancement of NPQ that reflects the dissipation of excess excitation energy in the form of harmless heat in young leaves (Figure 5a) at 30 min after spraying with CuZn NPs, could not protect young leaves from ROS generation at 30 min after the NPs spray (Figure 11b). However, the increase of NPQ in young leaves 90 min after the CuZn NPs spray (Figure 5a) was effective at retaining the same redox state of the PQ pool with control leaves and reducing H₂O₂ production at 90 min after the NPs spray to control levels (Figure 11c). An effective photoprotection can be attained only if NPQ is adjusted in such a way that no changes occur in the redox state of the PQ pool [41,59]. Otherwise, an imbalance between energy supply and demand occurs, indicating excess excitation energy [57–59]. Under such circumstances, the generation of H₂O₂ occurs (Figure 11b), which can be diffused through the leaf veins to act as a long-distance signaling molecule [38,41,60–62]. The intracellular ROS signaling pathways are initiated by the redox state of the PQ pool that regulates photosynthetic gene expression, comprising also a mechanism of plant acclimation [38,63,64]. The redox state of the PQ pool is of unique significance for antioxidant defense and signaling [65]. It has been shown recently that ROS generation is influenced also by the circadian system [66,67]. We postulate that ROS generation at 30 min after the NPs spray (Figure 11b) possibly served as the signaling molecule to contribute to a more oxidized state of the PQ pool at 90 min after the NPs spray (Figure 6, Figure 9c), resulting in a H₂O₂ production similar to the control leaf level (Figure 11c).

The foliar spray of *Arabidopsis thaliana* young and mature leaves with 30 mg L⁻¹ of CuZn NPs revealed a spatiotemporal heterogeneity of Φ_{PSII} and q_p measured (at 140 μmol photons m⁻² s⁻¹)

30 min, 90 min, 180 min, and 240 min after spraying (Figures 7–10). Young leaves show a higher spatial heterogeneity (Figures 7 and 9) compared to mature leaves (Figures 8 and 10). Nevertheless, PSII function was not uniform for both leaf types, making conventional chlorophyll fluorescence instruments not suitable for abiotic stress studies and pointing out the advantages of using chlorophyll fluorescence imaging analysis in the recognition of spatial heterogeneity at the leaf surface [29–35]. The response of cells to the same stress condition is not uniform, with some cells behaving more vulnerably than others [68].

In contrast to previous reports that young leaves acclimatize better to environmental changes and can maintain a better ROS homeostasis [43,45,69], mature leaves responded better. Thus, in disagreement with our hypothesis, the PSII photochemistry of young leaves seem to be negatively influenced when exposed to 30 mg L⁻¹ of CuZn NPs. Young leaves could overcome the negative effects on the function of PSII only after 240 min of the NPs spray, at which point the level of ROS accumulation was also similar to that of control young leaves. On the contrary, a beneficial effect was observed in the PSII function of mature leaves 30 min after the CuZn NPs spray, which was through an increased quantum efficiency of PSII photochemistry (Φ_{PSII}), an increased electron transport rate (ETR), an increased fraction of open PSII reaction centers (q_p), decreased ¹O₂ formation, and no notable changes in H₂O₂ generation.

Zinc and Cu are important micronutrients that are required for plant growth and development [1,38], but when they are in excess, they can cause toxicity effects on plant growth and development, affecting photosynthetic function [3,70]. In young leaves with sufficient Zn and Cu concentrations, the spray with 30 mg L⁻¹ of CuZn NPs resulted in an excess supply of them, causing negative effects on PSII function and increased ROS production. Increased H₂O₂ generation in young leaves after 30 min of spraying with 30 mg L⁻¹ of CuZn NPs (Figure 11b) was correlated to a lower oxidized state of the PQ pool (Figure 9b). Zinc is involved in a wide variety of physiological processes, playing catalytic, regulatory, and structural roles with several crucial functions in the cell [1,71–73], but excess Zn has to be detoxified in roots by sequestration to protect the sensitive photosynthetic leaf tissues [3,72]. Zn phytotoxicity varies extensively, depending on combinations with other heavy metals, the environmental conditions, the plant species, and the plant age [72], as well as by the leaf age, as shown here.

Leaf senescence turns leaves from units with a primary assimilation role into centers of nutrient mobilization [74,75]. During leaf senescence, new metabolic pathways are activated and others are de-activated, with nutrient and material remobilization, followed by a declining photosynthesis [74,75]. The *A. thaliana* rosette leaf 8 from six-week-old plants is a mature to senescing leaf; thus, nutrient remobilization occurs, resulting in nutrient deficiency. Spraying these leaves with 30 mg L⁻¹ of CuZn NPs restores Zn and Cu deficiency and improves photosynthetic efficiency. Zinc is known to contribute to the repair processes of PSII by turning over the photodamaged D1 protein [72,76]. Copper is vital for photosynthesis, and more than half of Cu is found in chloroplasts participating in the light reactions [77]. The foliar spraying of Cu NPs induced stress tolerance by stimulating antioxidant mechanisms [78]. However, this nutrient remobilization explanation has yet to be established.

Although plants are producers and play a key role in the ecosystem, the impact of NPs upon them is not well studied [79]. In order to understand the uptake, transport, and also bioaccumulation of NPs in plants after foliar exposure, different qualitative and quantitative methods are still being developed with an unclear comparability of results among the different techniques [80,81]. Among the different techniques, inductively coupled plasma mass spectroscopy (ICP-MS) is one of the most reliable methods for the detection of NPs, offering a range of advantages in high detection limits and high sensitivity for many elements [79,81–83].

Previously, both the positive and harmful impacts of NPs on terrestrial and aquatic plants have been established, which are mainly due to the concentration, size, and specific surface area of NPs, the exposure methodology, and the plant species that was examined [38,79,81,84–86]. In the root uptake of NPs, translocation to the above-ground parts takes place in a unidirectional pathway through

xylem vessels, while in the foliar uptake of NPs, translocation takes place in bidirectional pathways throughout the plant by the phloem [85]. The efficiency of uptake and translocation, and the effects of NPs on growth metabolism and photosynthesis vary from plant to plant [84]. Some studies report that the foliar application of NPs considerably increases the chlorophyll content in plants and results in a higher amount of light energy capture and photosynthesis enhancement [84], while another study reports that the root uptake of NPs decreases Φ_{PSII} and q_p , and increases Φ_{NO} due to an ineffective photoprotective mechanism (NPQ) resulting from a significant decrease of the PsbS protein, which is the key regulator of the energy dissipation process [87]. Nevertheless, the investigation on NPs is still at an initial phase; more laborious work is required in order to understand their impact on the physiological, biochemical, and molecular mechanisms in plants [79,84].

The present study demonstrates that considering the leaf developmental stage is important for understanding the mechanisms underlying leaf growth responses to environmental stresses [41–43,88]; thus, it must be taken into account in environmental stress studies in order to compare leaves of the same developmental stage [41–43,48,89]. Leaves of distinct ages differentially control stress responses, and plant responses against biotic and abiotic stresses are balanced in a leaf age-dependent manner [90].

Author Contributions: C.D.-S. and M.M. conceived and designed the experiments and analyzed the data; I.S., J.M., O.A. and I.-D.S.A. performed the experiments and analyzed the data; M.M. wrote the paper; all the authors review and approved the manuscript.

Funding: This research received no external funding.

Conflicts of Interest: The authors declare no conflict of interest.

References

1. Marschner, H. *Mineral Nutrition of Higher Plants*, 2nd ed.; Academic Press: London, UK, 1995.
2. Cakmak, I. Possible roles of zinc in protecting plant cells from damage by reactive oxygen species. *New Phytol.* **2000**, *146*, 185–205. [[CrossRef](#)]
3. Moustakas, M.; Bayçu, G.; Gevrek-Kürüm, N.; Moustaka, J.; Csatári, I.; Rognes, S.E. Spatiotemporal heterogeneity of photosystem II function during acclimation to zinc exposure and mineral nutrition changes in the hyperaccumulator *Noccaea caerulescens*. *Environ. Sci. Pollut. Res.* **2019**, *26*, 6613–6624. [[CrossRef](#)] [[PubMed](#)]
4. Alloway, B.J. Soil factors associated with zinc deficiency in crops and humans. *Environ. Geochem. Health* **2009**, *31*, 537–548. [[CrossRef](#)] [[PubMed](#)]
5. Ahmad, P.; Alyemeni, M.N.; Ahanger, M.A.; Wijaya, L.; Alam, P.; Kumar, A.; Ashraf, M. Upregulation of antioxidant and glyoxalase systems mitigates NaCl stress in *Brassica juncea* by supplementation of zinc and calcium. *J. Plant Interact.* **2018**, *13*, 151–162. [[CrossRef](#)]
6. Rameshraddy; Pavithra, G.J.; Rajashekar Reddy, B.H.; Mahesh, S.; Geetha, K.N.; Shankar, A.G. Zinc oxide nano particles increases Zn uptake, translocation in rice with positive effect on growth, yield and moisture stress tolerance. *Ind. J. Plant Physiol.* **2017**, *22*, 287–294. [[CrossRef](#)]
7. Doolette, C.L.; Read, T.L.; Li, C.; Scheckel, K.G.; Donner, E.; Kopittke, P.M.; Schjoerring, J.K.; Lombi, E. Foliar application of zinc sulphate and zinc EDTA to wheat leaves: Differences in mobility, distribution, and speciation. *J. Exp. Bot.* **2018**, *69*, 4469–4481. [[CrossRef](#)] [[PubMed](#)]
8. Cakmak, I. Enrichment of cereal grains with zinc: Agronomic or genetic biofortification? *Plant Soil* **2008**, *302*, 1–17. [[CrossRef](#)]
9. Prasad, R.; Shivay, Y.S.; Kumar, D. Agronomic biofortification of cereal grains with iron and zinc. *Adv. Agron.* **2014**, *125*, 55–91.
10. Garcia, P.C.; Rivero, R.M.; Ruiz, J.M.; Romero, L. The role of fungicides in the physiology of higher plants: Implications for defense responses. *Bot. Rev.* **2003**, *69*, 162–172. [[CrossRef](#)]
11. Zhao, L.; Huang, Y.; Hu, J.; Zhou, H.; Adeleye, A.S.; Keller, A.A. ¹H NMR and GC-MS based metabolomics reveal defense and detoxification mechanism of cucumber plant under nano-Cu stress. *Environ. Sci. Technol.* **2016**, *50*, 2000–2010. [[CrossRef](#)]
12. Ruttkey-Nedecky, B.; Krystofova, O.; Nejd, L.; Adam, V. Nanoparticles based on essential metals and their phytotoxicity. *J. Nanobiotechnol.* **2017**, *15*, 33. [[CrossRef](#)] [[PubMed](#)]

13. Servin, A.D.; White, J.C. Nanotechnology in agriculture: Next steps for understanding engineered nanoparticle exposure and risk. *NanoImpact* **2016**, *1*, 9–12. [[CrossRef](#)]
14. Liu, R.; Lal, R. Potentials of engineered nanoparticles as fertilizers for increasing agronomic productions. *Sci. Total Environ.* **2015**, *514*, 131–139. [[CrossRef](#)] [[PubMed](#)]
15. Parisi, C.; Vigani, M.; Rodríguez-Cerezo, E. Agricultural nanotechnologies: What are the current possibilities? *Nano Today* **2015**, *10*, 124–127. [[CrossRef](#)]
16. Moustaka, J.; Ouzounidou, G.; Sperdouli, I.; Moustakas, M. Photosystem II is more sensitive than photosystem I to Al³⁺ induced phytotoxicity. *Materials* **2018**, *11*, 1772. [[CrossRef](#)] [[PubMed](#)]
17. Anderson, J.M. Changing concepts about the distribution of photosystems I and II between grana-appressed and stroma-exposed thylakoid membranes. *Photosynth. Res.* **2002**, *73*, 157–164. [[CrossRef](#)]
18. Apostolova, E.L.; Dobrikova, A.G.; Ivanova, P.I.; Petkanchin, I.B.; Taneva, S.G. Relationship between the organization of the PSII supercomplex and the functions of the photosynthetic apparatus. *J. Photochem. Photobiol. B* **2006**, *83*, 114–122. [[CrossRef](#)]
19. Krause, G.H.; Weis, E. Chlorophyll fluorescence and photosynthesis: The basics. *Annu. Rev. Plant Physiol. Plant Mol. Biol.* **1991**, *42*, 313–349. [[CrossRef](#)]
20. Murchie, E.H.; Lawson, T. Chlorophyll fluorescence analysis: A guide to good practice and understanding some new applications. *J. Exp. Bot.* **2013**, *64*, 3983–3998. [[CrossRef](#)]
21. Kalaji, H.M.; Oukarroum, A.A.; Alexandrov, V.; Kouzmanova, M.; Brestic, M.; Zivcak, M.; Samborska, I.A.; Cetner, M.D.; Allakhverdiev, S.I. Identification of nutrient deficiency in maize and tomato plants by in vivo chlorophyll *a* fluorescence measurements. *Plant Physiol. Biochem.* **2014**, *81*, 16–25. [[CrossRef](#)]
22. Guidi, L.; Calatayud, A. Non-invasive tools to estimate stress-induced changes in photosynthetic performance in plants inhabiting Mediterranean areas. *Environ. Exp. Bot.* **2014**, *103*, 42–52. [[CrossRef](#)]
23. Moustaka, J.; Ouzounidou, G.; Bayçu, G.; Moustakas, M. Aluminum resistance in wheat involves maintenance of leaf Ca²⁺ and Mg²⁺ content, decreased lipid peroxidation and Al accumulation, and low photosystem II excitation pressure. *BioMetals* **2016**, *29*, 611–623. [[CrossRef](#)] [[PubMed](#)]
24. Kalaji, H.M.; Jajoo, A.; Oukarroum, A.; Brestic, M.; Zivcak, M.; Samborska, I.A.; Cetner, M.D.; Łukasik, I.; Goltsev, V.; Ladle, R.J. Chlorophyll *a* fluorescence as a tool to monitor physiological status of plants under abiotic stress conditions. *Acta Physiol. Plant.* **2016**, *38*, 1–11. [[CrossRef](#)]
25. Kitao, M.; Tobita, H.; Kitaoka, S.; Harayama, H.; Yazaki, K.; Komatsu, M.; Agathokleous, E.; Koike, T. Light energy partitioning under various environmental stresses combined with elevated CO₂ in three deciduous broadleaf tree species in Japan. *Climate* **2019**, *7*, 79. [[CrossRef](#)]
26. Guidi, L.; Lo Piccolo, E.; Landi, M. Chlorophyll fluorescence, photoinhibition and abiotic stress: Does it make any difference the fact to be a C3 or C4 species? *Front. Plant Sci.* **2019**, *10*, 174. [[CrossRef](#)] [[PubMed](#)]
27. Moustaka, J.; Panteris, E.; Adamakis, I.D.S.; Tanou, G.; Giannakoula, A.; Eleftheriou, E.P.; Moustakas, M. High anthocyanin accumulation in poinsettia leaves is accompanied by thylakoid membrane unstacking, acting as a photoprotective mechanism, to prevent ROS formation. *Environ. Exp. Bot.* **2018**, *154*, 44–55. [[CrossRef](#)]
28. Sperdouli, I.; Moustakas, M. Differential blockage of photosynthetic electron flow in young and mature leaves of *Arabidopsis thaliana* by exogenous proline. *Photosynthetica* **2015**, *53*, 471–477. [[CrossRef](#)]
29. Sperdouli, I.; Moustakas, M. Spatio-temporal heterogeneity in *Arabidopsis thaliana* leaves under drought stress. *Plant Biol.* **2012**, *14*, 118–128. [[CrossRef](#)]
30. Gorbe, E.; Calatayud, A. Applications of chlorophyll fluorescence imaging technique in horticultural research: A review. *Sci. Hortic.* **2012**, *138*, 24–35. [[CrossRef](#)]
31. Moustaka, J.; Moustakas, M. Photoprotective mechanism of the non-target organism *Arabidopsis thaliana* to paraquat exposure. *Pest. Biochem. Physiol.* **2014**, *111*, 1–6. [[CrossRef](#)]
32. Agathokleous, E.; Kitao, M.; Harayama, H. On the nonmonotonic, hormetic photoprotective response of plants to stress. *Dose-Response* **2019**, *17*, 1–3. [[CrossRef](#)] [[PubMed](#)]
33. Moustakas, M.; Malea, P.; Haritonidou, K.; Sperdouli, I. Copper bioaccumulation, photosystem II functioning and oxidative stress in the seagrass *Cymodocea nodosa* exposed to copper oxide nanoparticles. *Environ. Sci. Pollut. Res.* **2017**, *24*, 16007–16018. [[CrossRef](#)] [[PubMed](#)]
34. Bayçu, G.; Moustaka, J.; Gevrek-Kürüm, N.; Moustakas, M. Chlorophyll fluorescence imaging analysis for elucidating the mechanism of photosystem II acclimation to cadmium exposure in the hyperaccumulating plant *Noccaea caerulea*. *Materials* **2018**, *11*, 2580. [[CrossRef](#)] [[PubMed](#)]

35. Moustakas, M.; Malea, P.; Zafeirakoglou, A.; Sperdouli, I. Photochemical changes and oxidative damage in the aquatic macrophyte *Cymodocea nodosa* exposed to paraquat-induced oxidative stress. *Pest. Biochem. Physiol.* **2016**, *126*, 28–34. [[CrossRef](#)] [[PubMed](#)]
36. Cokoja, M.; Parala, H.; Schroter, M.K.; Birkner, A.; van den Berg, M.W.E.; Klementiev, K.V.; Grunert, W.; Fischer, R.A. Nanobrass colloids: Synthesis by Co-Hydrogenolysis of [CpCu(PMe₃)] with [ZnCp*₂] and investigation of the oxidation behaviour of a/b-CuZn nanoparticles. *J. Mater. Chem.* **2006**, *16*, 2420–2428. [[CrossRef](#)]
37. Schütte, K.; Meyer, H.; Gemel, C.; Barthel, J.; Fischer, R.A.; Janiak, C. Synthesis of Cu, Zn and Cu/Zn brass alloy nanoparticles from metal amidinate precursors in ionic liquids or propylene carbonate with relevance to methanol synthesis. *Nanoscale* **2014**, *6*, 3116–3126. [[CrossRef](#)] [[PubMed](#)]
38. Antonoglou, O.; Moustaka, J.; Adamakis, I.D.; Sperdouli, I.; Pantazaki, A.; Moustakas, M.; Dendrinou-Samara, C. Nanobrass CuZn nanoparticles as foliar spray non phytotoxic fungicides. *ACS Appl. Mater. Interfaces* **2018**, *10*, 4450–4461. [[CrossRef](#)] [[PubMed](#)]
39. Chang, Y.N.; Zhang, M.; Xia, L.; Zhang, J.; Xing, G. The toxic effects and mechanisms of CuO and ZnO nanoparticles. *Materials* **2012**, *5*, 2850–2871. [[CrossRef](#)]
40. Takahashi, S.; Badger, M.R. Photoprotection in plants: A new light on photosystem II damage. *Trends Plant Sci.* **2011**, *16*, 53–60. [[CrossRef](#)]
41. Moustaka, J.; Tanou, G.; Adamakis, I.D.; Eleftheriou, E.P.; Moustakas, M. Leaf age dependent photoprotective and antioxidative mechanisms to paraquat-induced oxidative stress in *Arabidopsis thaliana*. *Int. J. Mol. Sci.* **2015**, *16*, 13989–14006. [[CrossRef](#)]
42. Sperdouli, I.; Moustakas, M. A better energy allocation of absorbed light in photosystem II and less photooxidative damage contribute to acclimation of *Arabidopsis thaliana* young leaves to water deficit. *J. Plant Physiol.* **2014**, *171*, 587–593. [[CrossRef](#)] [[PubMed](#)]
43. Sperdouli, I.; Moustakas, M. Leaf developmental stage modulates metabolite accumulation and photosynthesis contributing to acclimation of *Arabidopsis thaliana* to water deficit. *J. Plant Res.* **2014**, *127*, 481–489. [[CrossRef](#)] [[PubMed](#)]
44. Agathokleous, E.; Mouzaki-Paxinou, A.C.; Saitanis, C.J.; Paoletti, E.; Manning, W.J. The first toxicological study of the antiozonant and research tool ethylene diurea (EDU) using a *Lemna minor* L. bioassay: Hints to its mode of action. *Environ. Pollut.* **2016**, *213*, 996–1006. [[CrossRef](#)] [[PubMed](#)]
45. Sperdouli, I.; Moustakas, M. Differential response of photosystem II photochemistry in young and mature leaves of *Arabidopsis thaliana* to the onset of drought stress. *Acta Physiol. Plant.* **2012**, *34*, 1267–1276. [[CrossRef](#)]
46. Jung, S. Variation in antioxidant metabolism of young and mature leaves of *Arabidopsis thaliana* subjected to drought. *Plant Sci.* **2004**, *166*, 459–466. [[CrossRef](#)]
47. Jiang, C.D.; Li, P.M.; Gao, H.Y.; Zou, Q.; Jiang, G.M.; Li, L.H. Enhanced photoprotection at the early stages of leaf expansion in field-grown soybean plants. *Plant Sci.* **2005**, *168*, 911–919. [[CrossRef](#)]
48. Bielczynski, L.W.; Łacki, M.K.; Hoefnagels, I.; Gambin, A.; Croce, R. Leaf and plant age affects photosynthetic performance and photoprotective capacity. *Plant Physiol.* **2017**, *175*, 1634–1648. [[CrossRef](#)]
49. Montag, J.; Schreiber, L.; Schonherr, J. An in vitro study on the post infection activities of copper hydroxide and copper sulfate against conidia of *Venturia inaequalis*. *J. Agric. Food Chem.* **2006**, *54*, 893–899. [[CrossRef](#)]
50. Balakumar, T.; Vincent, V.H.B.; Paliwal, K. On the interaction of UV-B radiation (280–315 nm) with water stress in crop plants. *Physiol. Plant.* **1993**, *87*, 217–222. [[CrossRef](#)]
51. Dillenburg, L.R.; Sullivan, J.H.; Teramura, A.H. Leaf expansion and development of photosynthetic capacity and pigments in *Liquidambar styraciflua*. *Am. J. Bot.* **1995**, *82*, 433–440. [[CrossRef](#)]
52. Demmig-Adams, B.; Adams, W.W., III. Photoprotection and other responses of plants to high light stress. *Annu. Rev. Plant Physiol. Plant Mol. Biol.* **1992**, *43*, 599–626. [[CrossRef](#)]
53. Demmig-Adams, B.; Adams, W.W., III; Barker, D.H.; Logan, B.A.; Bowling, D.R.; Verhoeven, A.S. Using chlorophyll fluorescence to assess the fraction of absorbed light allocated to thermal dissipation of excess excitation. *Physiol. Plant.* **1996**, *98*, 253–264. [[CrossRef](#)]
54. Klughammer, C.; Schreiber, U. Complementary PS II quantum yields calculated from simple fluorescence parameters measured by PAM fluorometry and the Saturation Pulse method. *PAM Appl. Notes* **2008**, *1*, 27–35.
55. Kasajima, I.; Ebana, K.; Yamamoto, T.; Takahara, K.; Yano, M.; Kawai-Yamada, M.; Uchimiya, H. Molecular distinction in genetic regulation of nonphotochemical quenching in rice. *Proc. Natl. Acad. Sci. USA* **2011**, *108*, 13835–13840. [[CrossRef](#)] [[PubMed](#)]

56. Gawroński, P.; Witoń, D.; Vashutina, K.; Bederska, M.; Betliński, B.; Rusaczek, A.; Karpiński, S. Mitogen-activated protein kinase 4 is a salicylic acid-independent regulator of growth but not of photosynthesis in Arabidopsis. *Mol. Plant* **2014**, *7*, 1151–1166. [[CrossRef](#)] [[PubMed](#)]
57. Müller, P.; Li, X.P.; Niyogi, K.K. Non-photochemical quenching. A response to excess light energy. *Plant Physiol.* **2001**, *125*, 1558–1566. [[CrossRef](#)] [[PubMed](#)]
58. Ruban, A.V. Nonphotochemical chlorophyll fluorescence quenching: Mechanism and effectiveness in protecting plants from photodamage. *Plant Physiol.* **2016**, *170*, 1903–1916. [[CrossRef](#)] [[PubMed](#)]
59. Lambrev, P.H.; Miloslavina, Y.; Jahns, P.; Holzwarth, A.R. On the relationship between non-photochemical quenching and photoprotection of photosystem II. *Biochim. Biophys. Acta* **2012**, *1817*, 760–769. [[CrossRef](#)]
60. Wilson, K.E.; Ivanov, A.G.; Öquist, G.; Grodzinski, B.; Sarhan, F.; Huner, N.P.A. Energy balance, organellar redox status, and acclimation to environmental stress. *Can. J. Bot.* **2006**, *84*, 1355–1370. [[CrossRef](#)]
61. Mittler, R.; Vanderauwera, S.; Suzuki, N.; Miller, G.; Tognetti, V.B.; Vandepoele, K.; Gollery, M.; Shulaev, V.; Van Breusegem, F. ROS signaling: The new wave? *Trends Plant Sci.* **2011**, *16*, 300–309. [[CrossRef](#)]
62. Baxter, A.; Mittler, R.; Suzuki, N. ROS as key players in plant stress signaling. *J. Exp. Bot.* **2014**, *65*, 1229–1240. [[CrossRef](#)] [[PubMed](#)]
63. Bräutigam, K.; Dietzel, L.; Kleine, T.; Ströher, E.; Wormuth, D.; Dietz, K.J.; Radke, D.; Wirtz, M.; Hell, R.; Dörmann, P.; et al. Dynamic plastid redox signals integrate gene expression and metabolism to induce distinct metabolic states in photosynthetic acclimation in Arabidopsis. *Plant Cell* **2009**, *21*, 2715–2732. [[CrossRef](#)] [[PubMed](#)]
64. Dietz, K.J.; Pfannschmidt, T. Novel regulators in photosynthetic redox control of plant metabolism and gene expression. *Plant Physiol.* **2011**, *155*, 1477–1485. [[CrossRef](#)] [[PubMed](#)]
65. Borisova-Mubarakshina, M.M.; Vetoshkina, D.V.; Ivanov, B.N. Antioxidant and signaling functions of the plastoquinone pool in higher plants. *Physiol. Plant.* **2019**, *166*, 181–198. [[CrossRef](#)] [[PubMed](#)]
66. Lai, A.G.; Doherty, C.J.; Mueller-Roeber, B.; Kay, S.A.; Schippers, J.H.M.; Dijkwel, P.P. CIRCADIAN CLOCK-ASSOCIATED 1 regulates ROS homeostasis and oxidative stress responses. *Proc. Natl. Acad. Sci. USA* **2012**, *109*, 17129–17134. [[CrossRef](#)] [[PubMed](#)]
67. Jones, M.A. Retrograde signalling as an informant of circadian timing. *New Phytol.* **2019**, *221*, 1749–1753. [[CrossRef](#)] [[PubMed](#)]
68. Stasolla, C.; Huang, S.; Hill, R.D.; Igamberdiev, A.U. Spatio-temporal expression of phytoglobin—A determining factor in the NO specification of cell fate. *J. Exp. Bot.* **2019**. [[CrossRef](#)]
69. Pinheiro, C.; Chaves, M.M. Photosynthesis and drought: Can we make metabolic connections from available data? *J. Exp. Bot.* **2011**, *62*, 869–882. [[CrossRef](#)]
70. Bayçu, G.; Gevrek-Kürüm, N.; Moustaka, J.; Csáti, I.; Rognes, S.E.; Moustakas, M. Cadmium-zinc accumulation and photosystem II responses of *Noccaea caerulea* to Cd and Zn exposure. *Environ. Sci. Pollut. Res.* **2017**, *24*, 2840–2850. [[CrossRef](#)]
71. Doncheva, S.; Stoyanova, Z.; Velikova, V. Influence of succinate on zinc toxicity of pea plants. *J. Plant Nutr.* **2001**, *24*, 789–804. [[CrossRef](#)]
72. Tsonev, T.; Lidon, F.J.C. Zinc in plants—An overview. *Emir. J. Food Agric.* **2012**, *24*, 322–333.
73. Caldelas, C.; Weiss, D.J. Zinc homeostasis and isotopic fractionation in plants: A review. *Plant Soil* **2017**, *411*, 17–46. [[CrossRef](#)]
74. Hoch, W.A.; Zeldin, E.L.; McCown, B.H. Physiological significance of anthocyanins during autumnal leaf senescence. *Tree Physiol.* **2001**, *21*, 1–8. [[CrossRef](#)]
75. Ougham, H.J.; Morris, P.; Thomas, H. The colors of autumn leaves as symptoms of cellular recycling and defenses against environmental stresses. *Curr. Top. Dev. Biol.* **2005**, *66*, 135–160.
76. Bailey, S.; Thompson, E.; Nixon, P.J.; Horton, P.; Mullineaux, C.W.; Robinson, C.; Mann, N.H. A critical role for the *Var2 FtsH* homologue of *Arabidopsis thaliana* in the photosystem II repair cycle in vivo. *J. Biol. Chem.* **2002**, *277*, 2006–2011. [[CrossRef](#)]
77. Hänsch, R.; Mendel, R.R. Physiological functions of mineral micronutrients (Cu, Zn, Mn, Fe, Ni, Mo, B, Cl). *Curr. Opin. Plant Biol.* **2009**, *12*, 259–266. [[CrossRef](#)]
78. Pérez-Labrada, F.; López-Vargas, E.R.; Ortega-Ortiz, H.; Cadenas-Pliego, G.; Benavides-Mendoza, A.; Juárez-Maldonado, A. Responses of tomato plants under saline stress to foliar application of copper nanoparticles. *Plants* **2019**, *8*, 151. [[CrossRef](#)]

79. Rastogi, A.; Zivcak, M.; Sytar, O.; Kalaji, H.M.; He, X.; Mbarki, S.; Brestic, M. Impact of metal and metal oxide nanoparticles on plant: A critical review. *Front. Chem.* **2017**, *5*, 78. [[CrossRef](#)]
80. Zhao, F.J.; Moore, K.L.; Lombi, E.; Zhu, Y.G. Imaging element distribution and speciation in plant cells. *Trends Plant Sci.* **2014**, *19*, 183–192. [[CrossRef](#)]
81. Deng, Y.; Petersen, E.J.; Challis, K.E.; Rabb, S.A.; Holbrook, R.D.; Ranville, J.F.; Nelson, B.C.; Xing, B. Multiple method analysis of TiO₂ nanoparticle uptake in rice (*Oryza sativa* L.) plants. *Environ. Sci. Technol.* **2017**, *51*, 10615–10623. [[CrossRef](#)]
82. Wu, B.; Becker, J.S. Imaging techniques for elements and element species in plant science. *Metallomics* **2012**, *4*, 403–416. [[CrossRef](#)]
83. Hanć, A.; Piechalak, A.; Tomaszewska, B.; Barańkiewicz, D. Laser ablation inductively coupled plasma mass spectrometry in quantitative analysis and imaging of plant's thin sections. *Int. J. Mass Spectrom.* **2014**, *363*, 16–22. [[CrossRef](#)]
84. Kataria, S.; Jain, M.; Rastogi, A.; Zivcak, M.; Brestic, M.; Liu, S.; Tripathi, D.K. Role of nanoparticles on photosynthesis: Avenues and applications. In *Nanomaterials in Plants, Algae and Microorganisms: Concepts and Controversies*; Tripathi, D.K., Ahmad, P., Sharma, S., Chauhan, D.K., Dubey, N.K., Eds.; Elsevier, Academic Press: Cambridge, MA, USA, 2019; Volume 2, pp. 103–127.
85. Hussain, I.; Singh, A.; Singh, N.B.; Singh, A.; Singh, P. Plant-nanoceria interaction: Toxicity, accumulation, translocation and biotransformation. *S. Afr. J. Bot.* **2019**, *121*, 239–247. [[CrossRef](#)]
86. Malea, P.; Charitonidou, K.; Sperdouli, I.; Mylona, Z.; Moustakas, M. Zinc uptake, photosynthetic efficiency and oxidative stress in the seagrass *Cymodocea nodosa* exposed to ZnO nanoparticles. *Materials* **2019**, *12*, 2101. [[CrossRef](#)]
87. Chen, Y.; Wu, N.; Mao, H.; Zhou, J.; Su, Y.; Zhang, Z.; Zhang, H.; Yuan, S. Different toxicities of nanoscale titanium dioxide particles in the roots and leaves of wheat seedlings. *RSC Adv.* **2019**, *9*, 19243–19252. [[CrossRef](#)]
88. Pantin, F.; Simonneau, T.; Muller, B. Coming of leaf age: Control of growth by hydraulics and metabolics during leaf ontogeny. *New Phytol.* **2012**, *196*, 349–366. [[CrossRef](#)]
89. Majer, P.; Hideg, É. Developmental stage is an important factor that determines the antioxidant responses of young and old grapevine leaves under UV irradiation in a green-house. *Plant Physiol. Biochem.* **2012**, *50*, 15–23. [[CrossRef](#)]
90. Berens, M.L.; Wolinska, K.W.; Spaepen, S.; Ziegler, J.; Nobori, T.; Nair, A. Balancing trade-offs between biotic and abiotic stress responses through leaf age-dependent variation in stress hormone cross-talk. *Proc. Natl. Acad. Sci. USA* **2019**, *116*, 2364–2373. [[CrossRef](#)]



© 2019 by the authors. Licensee MDPI, Basel, Switzerland. This article is an open access article distributed under the terms and conditions of the Creative Commons Attribution (CC BY) license (<http://creativecommons.org/licenses/by/4.0/>).